Electronic Supplementary Material

Section A - documentation of routes definitions in Flee

The routes.csv input file, determining the connections in the location graph, consists of four columns: Name1, Name2, Distance [km] and forced_redirection. Location A and B mark the start and end point of a route respectively. Distance displays the distance of the route in km, and also it acs as a weighting factor. For instance, in cases where the travel takes twice as long, due to traffic congestion, this distance value would be doubled. The forced_redirection column refers to a redirection from a source location, which can be a town or a camp, to a destination location. The source location is then indicated as a forwarding hub. In this column, the value 0 indicates no redirection, while 1 indicates redirection from Name2 to Name1, and 2 indicates redirection from Name1 to Name2. The implementation of the new routes, which take into account the seasonal changes in weighted route length, require the splitting-up of the Distance column into four seasons. Flee has been updated to do so, where the connection between two locations can differ in length in different seasons. Table ESMA1 and ESMA2 show the schematic overview of the routes.csv structure, the original and the updated version, respectively.

Table ESMA1. Routes.csv original file structure.

Name1	Name2	Distance	Forced_redirection
A	B	X1	0
B	C	X2	1

Table ESMA2. Routes.csv adapted file structure.

Name1	Name2	DistanceS1	DistanceS2	DistanceS3	DistanceS4	Forced_redirection
A	B	X11	X12	X13	X14	0
B	C	X21	X22	X22	X24	1

Section B - additional technical details on cost raster creation

The *Soil* data in Mali, which in this case is represented by the term surface, is reduced to three classes, besides open water and wetlands, which are explained in different sections. These three classes are *compacted sand/gravel/grassland, loose sand* and *rocky areas*. To delineate these classes in the terrain, two methods are used. The first method is to reclassify the Esri Land Cover 2020 dataset, which consists of a raster with a 10-meter resolution and its areas are divided into 10 classes, derived from Sentinel 2 data. This dataset is used for each season, as it is assumed that the used land cover features do not change seasonally. Through visual inspection, loose sand is assumed to form the 'bare areas' class in the Esri dataset. All other classes in the dataset are reclassified to form the *compacted sand/gravel/grassland* class. The data are then aggregated to a 30-meter resolution dataset, to match the other datasets used in the study.

Table ESM1. Summary of data used in the study.

Type	Feature	Data
Relief	Slope – percentage of incline – non-seasonal feature	JAXA ALOS Global 30m DSM (2021)
Drainage	Presence of open water and wetlands / floodplains – seasonal feature	Sentinel 2 – Indexed satellite images (NDMI / Wetlands in Water (WiW))
Soil	Surface material – loose sand, rocky surfaces and compacted sand/gravel/grassland– partially seasonal feature	Sentinel 2 - Esri Land Cover 2020
Infrastructure	Presence of roads, bridges, ferries or fordable river sections – partially seasonal feature	Open Street Map; Esri Land Cover (2020)

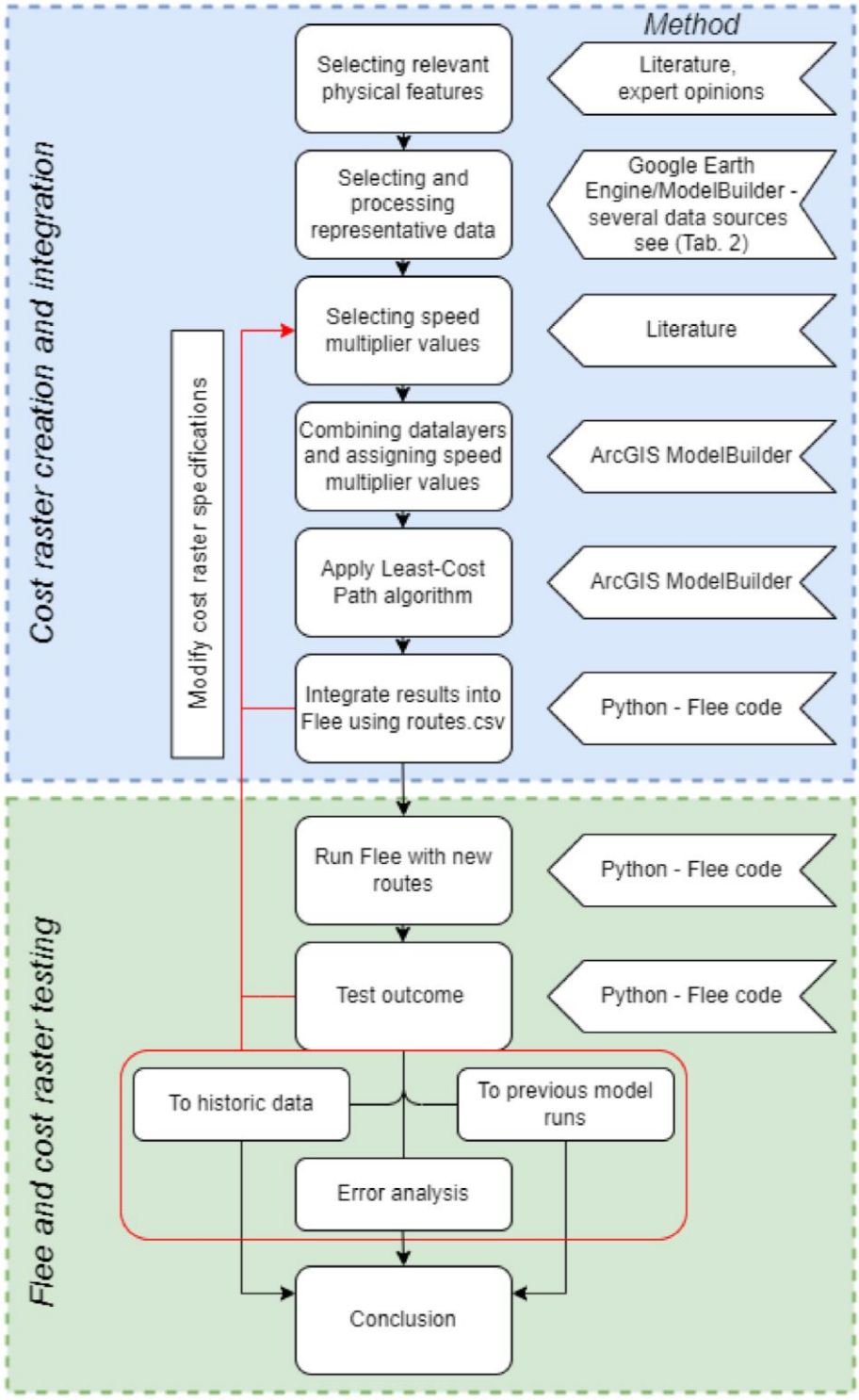

Figure ESM1. Schematic overview of the Cost Raster Creation methodology.

The *Soil* data in Mali, which in this case is represented by the term surface, is reduced to three classes, besides open water and wetlands, which are explained in different sections. These three classes are *compacted sand/gravel/grassland, loose sand* and *rocky areas*. To delineate these classes in the terrain, two methods are used. The first method is to reclassify the Esri Land Cover 2020 dataset, which consists of a raster with a 10-meter resolution and its areas are divided into 10 classes, derived from Sentinel 2 data. This dataset is used for each season, as it is assumed that the used land cover features do not change seasonally. Through visual inspection, loose sand is assumed to form the 'bare areas' class in the Esri dataset. All other classes in the dataset are reclassified to form the *compacted sand/gravel/grassland* class. The data are then aggregated to a 30-meter resolution dataset, to match the other datasets used in the study.

The rocky areas are derived through a random forest supervised classification of satellite images. This method is proven to yield accurate results when used for defining land cover classification [1,2] The *rocky areas* class is meant to delineate a phenomenon in Mali where patches of sharp, jagged rocks cover the surface. From personal communication, it is found that these surfaces are virtually impassable for civilian vehicles, as the rocks have the ability to destroy tires (B. Ooink, personal communication, September 2021). These dark patches are distinguishable from space. Therefore, random forest supervised classification allows for sharp demarcation of these areas. The rocky areas are set to *NoData*, using the *Set Null* tool, where the presence of rocks is set to *NoData.* This allows further calculations to take place, without taking the rocky areas into account, as these are un-traversable. To the bare and rest dataset a speed multiplier (*ResVal*) class is added. These classes are defined through a reclassification of a predefined land.

The presence of water or wetlands represents *Drainage*, where the seasonal presence of water is set to *NoData* to represent an impassable surface. The yearly dataset, which are multi-spectral images from ESA Copernicus' Sentinel 2 1C mission, denotes the locations of dried up wetlands, or floodplains. The cells of this dataset are set to the determined speed multiplier values as well. We use the Normalized Difference Water Index (NDWI) method proposed by McFeeters [3] to derive the water data. In remote sensing, NDWI may refer to several different indexing methods. This method is created specifically to delineate land from open water using light in the green and near-infrared (NIR) wavelengths [4]. Moreover, a study by Özelkan [5] has shown that the NDWI method is the most suitable method for detecting water bodies in comparison to several other methods developed for this purpose. Equation 1 shows the formula for McFeeters' NDWI.

$$NDWI = \frac{(-NIR)}{(+NIR)} \tag{1}$$

The NDWI yields a dataset with values between 1 and -1. As a general rule, positive values depict water [5–7]. This is caused by the relatively high reflectance of NIR light by soil and terrestrial vegetation [5].

While the NDWI is ideal for detecting open water bodies, it is not suitable for measuring moisture levels in soil or wetlands. In general, the remote sensing of wetlands provides a difficult challenge to researchers [8]. This is mainly due to the dynamic nature and ambiguous definition of wetlands [9], which constantly change [10]. Furthermore, measuring moisture levels under an obstructing layer of vegetation is challenging as well. However, the *Water in Wetlands* (WiW) is a relatively new method, published by Lefebvre et al. [11], which uses a relatively simple calculation to distinguish wet- from dryland (Equation 2).

$$Wetland = NIR \leq 0.1804 \wedge SWIR \leq 0.1131 \tag{2}$$

In Equation 2, near-infrared (NIR) and shortwave-infrared (SWIR) are combined. SWIR is used, as it is sensitive to moisture both in soils and in vegetation [11,8]. If the reflectance value of a pixel is lower than 0.1804 in the NIR band, and it is lower than 0.1131 in the SWIR band, the pixel should be classified as wetland. The values in this formula are specified to best suit Sentinel 2 data. To apply the NDWI and WiW methods, satellite imagery that includes at least RGB, NIR and SWIR bands should be used.

Copernicus' Sentinel 2 data are useful for this study due to several reasons. Firstly, the Sentinel 2 mission retrieves high spatial-resolution images in several different bands. These bands include visible light and near-infrared light, which makes the data suitable for NDWI calculations. Secondly, the temporal resolution of the data is high. The revisit time of the Sentinel 2 satellites is approximately five days. This allows for comparing the signal over time and detecting seasonal change accurately. To do this, the data is first classified into four seasons. The start and end dates of these seasons can be found in Table ESM2. The dry season marks the period where the Niger river is at its largest. The water upstream arriving with a delay downstream causes this. This period falls generally between October and March, so from seasons 1 through 4. The wet season ranges roughly from April through September, in seasons 2 and 3. In this period, the water volume in the Niger is at its lowest.

Table ESM2. Dates used for seasonal reclassification

Dates used for seasonal reclassification of Sentinel data		
Seasons	Start date	End date
Season 1	1st of January	31st of March
Season 2	1st of April	30th of June
Season 3	1st of July	31st of September
Season 4	1st of October	31st of December

The data class *Infrastructure* consists of several road features. The *roads* dataset is derived from OSM, an open-source infrastructure data source that is frequently updated. The OSM database is accessed by using the QGIS plug-in QuickOSM. *Infrastructure* class split into roads and river crossing. Roads are classified into five types (primary roads, secondary roads, tertiary roads, residential roads and unclassified roads) and river crossings classified into three types.

Furthermore, in the OSM data several properties in the roads dataset are included that are important to simulating the situation in Mali. This is the case periodically in Mali due to the significant changes in water flows. Some routes of travel are not viable in one season, while they are in another season, due to the swelling and shrinking of the rivers. These properties include the presence of bridges, ferries and fordable areas. It is assumed that vehicles used by refugees do not have the capability to traverse open water, and are therefore reliant on these crossings. To select bridges, road sections where the property *bridges* equals *T* (for 'True'), are stored in a separate file. The same is done for the property *ford*, which indicates a fordable area. Next, to select ferries, the point dataset 'Ferry terminals' is taken. To include ferries in the road network, vertices were manually drawn between the ferry terminals and the nearest road. Some 40 ferry connections exist in Mali according to OSM, with an additional 26 in the buffer area. To ensure the connection would transfer correctly to raster data, the river crossings were buffered using the *Buffer* function, with a diameter of 90 meters, or roughly three cells. All data are then converted to raster using the ArcGIS Pro tool *Feature to Raster* to allow for the inclusion of the data in the model.

River crossings are buffered by 45 meters, resulting in a diameter of 90 meters around the river crossings, or roughly three cells. This is done to prevent connections getting lost in future data transformations, mainly from vector to raster data. The roads and river crossing data assign their speed multiplier values subsequently. The result is eight raster datasets representing the infrastructure. To use these data correctly in the model, there are some assumptions. First, due to the periodically low water level, ferries are only usable in high river levels. Second, due to the periodically high water levels, fordable areas are only usable in low river levels. Finally, bridges are always usable. The designed model represents the relations between the infrastructure and the seasonally different environment.

After the datasets are in their correct state, they are added together using several operations. In the initial situation, all cells in the study area are valued at 1. The first step is to subtract all impassable surfaces from the area. This is done by multiplying the 'Value1'. The next step is to assign speed multiplier values to the remaining cells. The land cover data is taken into account, by multiplying the speed multiplier values with the previously created raster. Now all cells have either a *NoData* or land cover speed multiplier value. After this, the yearly wetlands are added by replacing the previous speed multiplier values, if the floodplain value is lower. In the absence of floodplains, the speed multiplier value of the land cover is used. Finally, the roads are overlaid, ignoring the previous operations when a road is present, and assigning the road speed multiplier value to the cell.

In the periods when the Niger river is generally at its peak volume, in seasons one and four, fords are made inaccessible in the model. The opposite is true for ferries, which are not accessible in seasons two and three, when the river is reduced in size and volume. Bridges are available throughout the seasons. This results in the need to take different routes in different seasons, as some river crossings become inaccessible.

For the *Relief* data class, it needs to assign the values of slope speed multiplier, as they affect roads as well. Slope data, derived from a Digital Elevation Model (DEM), represents the percentage of incline between different elevations and is derived from the Japanese space agency's ALOS global digital surface model. The aspect, or the orientation of the slope, is not taken into account when deciding the degree of resistance that the slope offers. The slope data has five classes, each with their own speed multiplier value. However, as the slopes directly influence speed, the cells have to be changed from an arbitrary speed multiplier value to km/h by multiplying the entire raster by a maximum speed value. When the cells represent speed, they are adjusted to the speed multiplier effect of the slope, in accordance with the assigned speed multiplier classes.

Using our representation of the physical environment, we can now complete the speed raster creation and convert it into a cost raster, representing the required time to travel one meter in the cell. This is done using Equation 3, where *SpeedValue* is the value assigned to each cell of the raster. The formula returns the cost in hour/meter. The transformation to cost raster is necessary for the Least Cost Path operation. To finalize the creation of the cost raster, and to reduce processing time and storage requirements, the raster is resampled from a horizontal resolution of ~30x30m to 100x100 meters, using the minimum value of the aggregated cells. This method ensures that roads and river crossings remain represented in the raster. To create the cost raster, we use

the ArcGIS Pro ModelBuilder, which allows easy adoption of changes and repetition of the model. Furthermore, it provides a visual overview of the complete model. Figure 7 depicts a schematic overview of these steps, including the details of the operations.

$$Cost = \left(\frac{1}{SpeedValue}\right) * 0.001 \quad (3)$$

*Surface speed multiplier values: t*he speed multiplier values for different surface materials are determined using literature sources. As no single source is found that described the needed values completely, the values used for this study are a combination of several studies. The values for roads and open water are not determined from literature. It is assumed that maximum speed can be obtained on roads, as these are usually the paths of least resistance for vehicles. This maximum speed value is already adapted to the quality of roads in the study area. Water is given the value 0, representing an impassable object. In the table, wet and dry seasons are given different values, as some terrain surfaces might be affected by this fluctuation. Table ESM3 summarizes the values derived from the literature for all surface classes in both wet and dry seasons.

Table ESM3. Speed multiplier values summarized

Feature	Baylot *et al.*, 2005		Malm, 2019		Rybanský, 2003	
	Dry season	Wet season	Dry season	Wet season	Dry season	Wet season
Compacted sand/gravel/grassland	0.7	0.7	0.8	0.6	1	1
Loose sand	0.85	0.85	0.6	0.8	0.5	0.5
Rocky surface	0	0	NA	NA	0	0
Wetlands	0	0	0	0	0	0
Floodplain	0.85	0.85	0.2	0	0.5	0.5

The mean is calculated on the values listed in Table ESM3. However, testing has shown that these values are still high, and might provide a distorted image of reality, in comparison to the road speed multipliers. Besides the physical resistance of surfaces, there are several components that play a role in the actual accessibility of surfaces as well. First, off-road surfaces are less accessible not only due to the soil structure, but also due to land-cover objects. Second, there is a mental factor at play. If provided with a choice, people will most likely pick a path or trail over an area devoid of visible routes, even though it might take more time. Furthermore, there is a factor of not knowing how much longer it will take to drive along a road instead of going off-road. These factors are difficult to quantify. It is assessed that the extra resistance factors will amount to a further decrease of roughly 50% of the speed multiplier values. The results of this are displayed in Table ESM4.

Table ESM4. Final speed multiplier values

Feature	Speed multiplier values	
	Dry season	Wet season
Roads	see Table XX	see Table 9
Compacted sand/gravel/grassland	0.4	0.4
Loose sand	0.3	0.3
Rocky surface	0	0
Wetlands	0.5 (when dry)	0 (when wet)
Water	0	0

The road data speed multiplier values are split up into several classes (Table ESM5). This is done to represent the different quality of different road types. The values range from 1 to 0.8. The lower value, 0.8, is set to not go below the least resistant non-road surface, which is compacted sand/gravel/grassland. With the exception of river crossings, all road speed multipliers are either equal to or higher than 0.8. The first class, primary roads, represents national highways. This class is set to 1, representing that these roads allow for the maximum speed to be obtained [12]. Secondary roads represent regional roads. Visual inspection of the dataset shows that some of these roads are paved, but are of lesser quality in comparison to the primary roads. Therefore, the speed multiplier value of this layer is slightly increased. Tertiary and residential roads are assigned the same value. These local or regional roads are either of lesser quality or reduce maximum speed through traffic regulations. The value is therefore 0.9 [12]. Unclassified roads can be any road or path that cannot be assigned to a specific class. These roads do not allow much faster travel than some roadless areas. The difference is therefore only 0.05 to compacted sand/gravel/grassland.

The river crossing classes are classified separately. Of the three classes, 'bridges' allows for faster travel. Some bridges might be more narrow than the connecting roads, and therefore demand a significant slowdown. Fords slow down more, to represent having to drive carefully through an inundated area, reducing the speed by 80% in this case. Ferries have the lowest speed multiplier, representing waiting time for the ferry to arrive, and slow transport across the waterbody.

Table ESM5. Road speed multiplier values

Road class	Speed multiplier values
Primary roads	1
Secondary roads	0.95
Tertiary roads	0.90
Residential roads	0.90
Unclassified roads	0.85
Bridges	0.50
Fords	0.20
Ferries	0.10

*Slope speed multiplier values: t*he speed multiplier values for different slope angles are derived from literature as well. The method described by Shoop et al. [13] is a simplified classification derived from the NRMM method [14]. It defines five classes of slopes, each of which gets assigned a speed multiplier value [13,15]. The maximum slope in this method is 30%. Slopes above this angle are classified as no go terrain. However, the values described by Shoop et al. are meant to represent military vehicles, which are often suited for rough terrain and equipped with four-wheel drive capabilities. Therefore, the values for this case study are adjusted to represent the wide range of vehicles that might be used by refugees. The speed multiplier value is increased to represent this difference in vehicle power and capabilities. The classes, values and slowdown factors are listed in Table ESM6. The values that will be used in the raster are listed under the *adjusted speed multiplier factor.*

Table ESM6. Slope speed multiplier values, derived from Shoop *et al.* [13]

Slope class (%)	Speed reduction percentage	Speed multiplier value	Adjusted speed multiplier value
0 – 5	0%	1	1
5 – 15	10%	0.9	0.8
15 – 25	20%	0.8	0.6
25 – 30	30%	0.7	0.4
>30	NoGo / 100%	0	0

Route creation and implementation: After the cost raster, the next step is to create new routes by using the Least-Cost Path algorithm for the Flee model. To do this, the data need to be transformed to a projected coordinate system that uses metric units. To minimize projection-induced distortion, we choose the projected coordinate system WGS 1984 Web Mercator (Auxiliary Sphere). Furthermore, the Mercator projection increasingly distorts land area and distance towards the poles, but remains accurate around the equator, which is where our case study is located. To create the routes, first, start points and destinations have to be defined based on ACLED and UNHCR data. Then, we find the route between these locations using data on existing road connections, OSM Services, and local knowledge of the region.

To create least cost path routes across the created cost surfaces, two additional rasters have to be created per route: a backlink raster and a cost distance raster. Both can be created using the Cost Distance tool in ArcGIS Pro. This tool requires two inputs: the cost surface and the source data, or start location. The cost distance raster identifies, for each cell, the least accumulative cost distance over a cost surface of the identified source location, in hours per meter. The resulting raster contains data for each cell on the least cost, not Euclidean distance, to the source location. Figures ESM2 and ESM3 show the examples of both rasters, using Ségou as a source location.

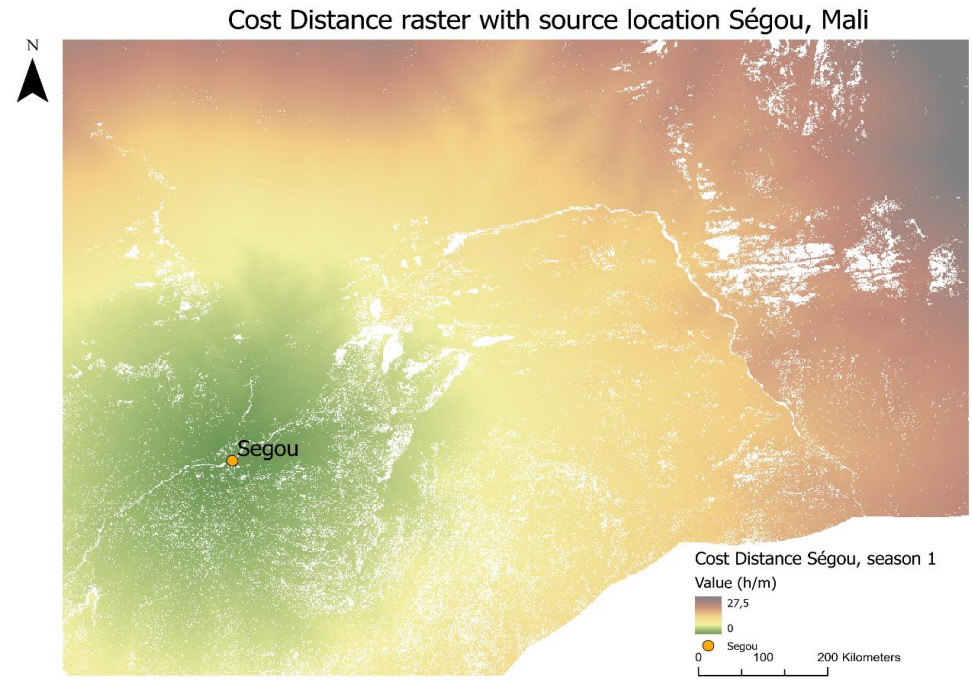

Figure ESM2. Cost Distance raster for Ségou, Mali.

The backlink raster defines the direction or identifies the next neighboring cell along the least accumulative cost path from a cell to reach its least-cost source. It contains values ranging from 0 to 8, each representing different directions (right, lower-right, down, etc.) (Figure ESM3).

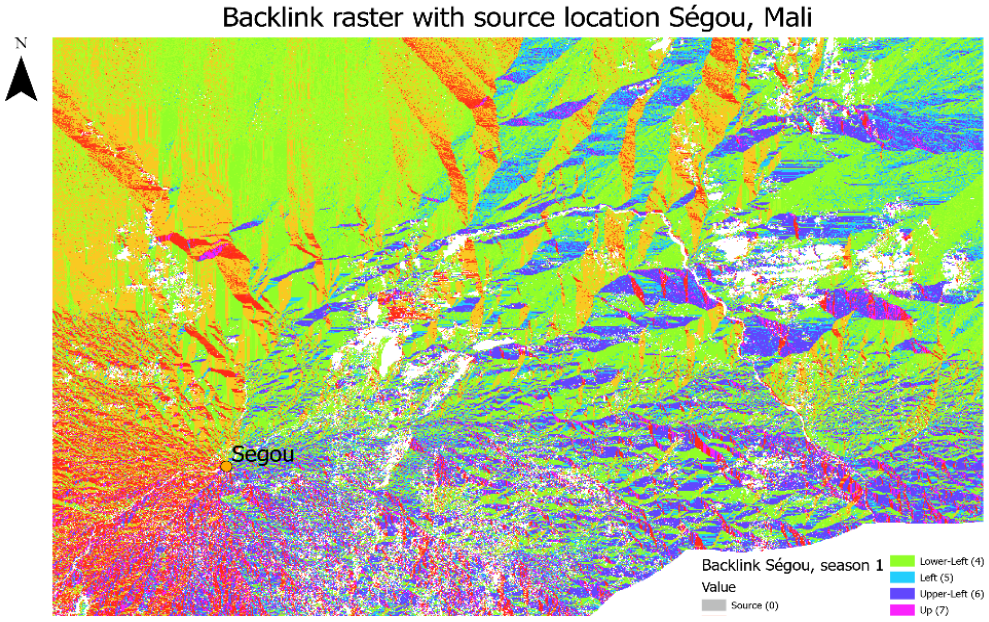

Figure ESM3. Backlink raster for Ségou, Mali.

After that, the calculation of the least-cost path can begin. The tool used for this is the Cost Path as Polyline tool in ArcGIS Pro. This tool takes three datasets as input: the destination point data, a cost distance raster and a backlink raster. The tool calculates the least-cost path between the source cell used for creating the cost distance and backlink rasters. It returns a polyline feature, with an attribute representing the accumulative cost of the represented route in hours.

The final step is to transform the cost of the routes to a weighted distance. This is required for the route representation in the Flee model. To do this, the cost in hours needs to be represented as kilometers as a weighting factor, which will be multiplied by the Euclidean distance of the route. First, the geometry of the route needs to be calculated. This is done using the tool Calculate Geometry Attributes, which allows the

creation of a new field and the filling of this field in one tool. To get the weighting factor, the speed difference needs to be known: the Euclidean length of the route is divided by the maximum speed, which in this case is 80 km/h. The length of the route divided by 80 results in the required time to drive the route with the maximum speed. Now two time measurements are known for the route, the path cost, as derived from the Cost Path tool, and the cost surface divided by the time, resulting from the maximum speed calculation. The result, which should be greater than one and provide the weighting multiplier, multiplied by the Euclidean route length to calculate the weighted distance (Equation 4).

$$WeightedDistance = \frac{RouteCost}{\left(\frac{RouteLength}{MaxSpeed}\right)} * RouteLength \quad (4)$$

Section C: Full table to route weights over time, using the DPEN.

Table ESM7. List of link weights by season defined in our Flee simulation, based on the results of our DPEN model. Differences are compared to the originally defined weights in Flee, which were static and solely based on distance.

Location A	Location B	New distance, season 1	New distance, season 2	New distance, season 3	New distance, season 3	Old distance	Average Difference (%)
Abala	*Menaka*	216,21	216,21	216,21	216,21	172	25,7%
Abala	*Niamey*	275,27	275,27	275,27	275,27	253	8,8%
Ansongo	*Gao*	124,41	120,33	120,33	124,41	100	22,4%
Ansongo	*Menaka*	271,07	271,07	271,07	271,07	191	41,9%
Bobo Dioulasso	*Bamako*	628,28	628,28	628,28	628,29	-	
Bobo Dioulasso	*Mentao*	535,99	535,99	535,99	535,99	475	12,8%
Bobo Dioulasso	*Mopti*	534,76	534,65	534,76	535,28	462	15,8%
Bobo Dioulasso	*Segou*	479,59	470,33	483,49	479,6	376	27,2%
Bourem	*Gao*	104,46	104,46	104,46	104,46	97	7,7%
Bourem	*Timbuktu*	455,05	455,05	455,05	455,05	314	44,9%
Douentza	*Gao*	458,69	458,69	458,69	458,69	397	15,5%
Douentza	*Konna*	129,17	129,17	129,17	129,17	121	6,8%
Douentza	*Mentao*	271,64	271,64	271,64	271,64	487	-44,2%
Douentza	*Timbuktu*	274,18	993,6	1017,87	288,13	-	
Goundam	*Diré*	40,34	40,28	40,28	40,34	42	-4,0%
Goundam	*Niafunké*	96,24	96,24	96,24	96,24	78	23,4%
Goundam	*Timbuktu*	99,3	99,3	99,3	99,3	85	16,8%
Kidal	*Ansongo*	527,64	523,57	523,57	527,64	-	
Kidal	*Bourem*	329,59	329,59	329,59	329,59	308	7,0%
Kidal	*Gao*	410	410	410	410	-	
Kidal	*Menaka*	420,6	420,6	420,6	420,6	-	
Konna	*Mopti*	75,48	75,48	75,48	79,98	70	9,4%
Konna	*Niafunké*	573,86	929,43	945,46	589,68	153	396,5%
Konna	*Timbuktu*	392,15	1122,52	1140,15	406,1	303	152,6%
Léré	*Fassala-Mbera*	155,67	155,67	155,67	155,67	98	58,8%
Léré	*Niafunké*	153,06	139,62	139,63	139,63	140	2,1%
Léré	*Ténenkou*	232,57	232,57	232,57	232,57	295	-21,2%
Mangaize	*Abala*	259,78	259,78	259,78	259,78	256	1,5%
Mangaize	*Menaka*	200,57	200,57	200,57	200,57	305	-34,2%
Mangaize	*Niamey*	171,97	171,97	171,97	171,97	159	8,2%
Mangaize	*Tabareybarey*	174,23	174,06	174,06	174,23	217	-19,7%
Mentao	*Ansongo*	445,25	563,68	564,57	448,09	-	
Mentao	*Mopti*	386,67	386,67	386,67	391,18	360	7,7%
Mentao	*Niamey*	512,6	512	510,45	512,6	-	
Mentao	*Tabareybarey*	580,7	418,16	554,17	583,54	-	
Niafunké	*Ténenkou*	380,14	354,52	354,27	369,66	308	18,4%
Segou	*Bamako*	269,04	269,04	269,04	269,04	240	12,1%
Segou	*Fassala-Mbera*	387,66	387,66	387,66	387,72	-	
Segou	*Mopti*	342,47	365,09	385,74	373,5	401	-8,6%
Segou	*Ténenkou*	255,24	255,85	256,59	255,87	228	12,2%
Tabareybarey	*Abala*	415,11	415,11	415,11	415,11	412	0,8%
Tabareybarey	*Ansongo*	161,63	161,63	161,63	161,63	148	9,2%
Tabareybarey	*Menaka*	346,66	346,66	346,66	346,66	361	-4,0%
Tabareybarey	*Niamey*	224,69	224,69	224,69	224,69	205	9,6%

Section D: Graphical Overview of the Cost Raster Creation Process

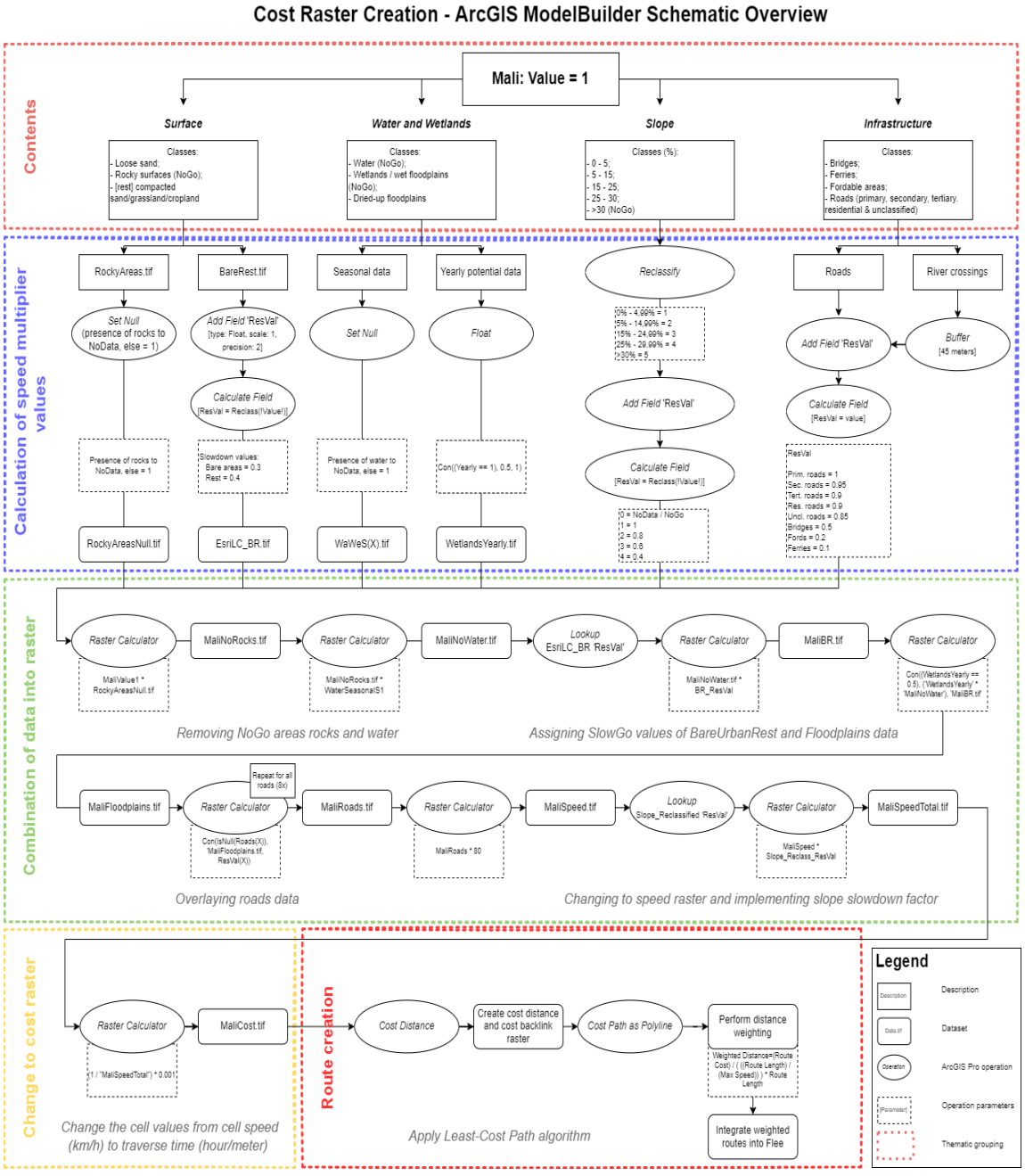

Figure ESM4. Schematic overview of cost raster creation.

Section E: Full table of RMSE and NRMSE values

Values are by camp, averaged over 10 runs. A negative difference indicates an improvement compared to the old static route weight calculation approach.

Table ESM8. Normalized RMSE by camp location. Difference indicates to what extent the inclusion of the DPEN modelling results resulted in an improvement (negative) or reduction (positive) of the NRMSE score for that location.

Location	Old route mean normalized RMSE	New route mean normalized RMSE	Difference
Fassala-Mbera	0.26	0.24	-0.023
Mentao	0.18	0.22	0.035
Bobo-Dioulasso	0.31	0.30	-0.006
Abala	0.13	0.15	0.021
Mangaize	0.14	0.22	0.080
Niamey	0.62	0.57	-0.047
Tabareybarey	0.43	0.42	-0.008
Total	0.15	0.13	-0.025

Below we also provide the direct comparison of refugee arrivals for the various camps. This data has been used to calculate the RMSE, NRMSE and ARD values (latter are mentioned in the main manuscript as well as in [16,17]).

Figure ESM5. Average refugee arrival numbers per location.

References

1. Gallant, A.L. The Challenges of Remote Monitoring of Wetlands. *U.S. Geological Survey*, **2015**, *7*, 10938–10950. https://doi.org/10.3390/rs70810938.
2. Gislason, P.O., Benediktsson, J.A., Sveinsson, J.R. Random Forests for land cover classification. *Department of Electrical and Computer Engineering*, 2005, *2*. https://reader.elsevier.com/reader/sd/pii/S0167865505002242?token=5D0B53237D37D967CD86A8D6CBBF37A4F5E8C4CE48E38DAD5E94752C5FE01F6955D035777F1CACC9A46808067616E63F&originRegion=eu-west-1&originCreation=20211201134216.
3. McFeeters, S.K. The use of the Normalized Difference Water Index (NDWI) in the delineation of open water features, **1996**, *17*, 1425–1432. https://doi.org/10.1080/01431169608948714

4. Eid, A.N.M., Olatubara, C.O., Ewemoje, T.A., El-Hennawy, M.T., Farouk, H. Inland wetland time-series digital change detection based on SAVI and NDWI indecies: Wadi El-Rayan lakes, Egypt. *Remote Sensing Applications: Society and Environment*, 2020,*19*. https://doi.org/10.1016/j.rsase.2020.100347
5. Özelkan, E. Water Body Detection Analysis Using NDWI Indices Derived from Landsat-8 OLI. *Polish Journal of Environmental Studies*, **2020**, *29*, 1759–1769. https://doi.org/10.15244/PJOES/110447.
6. Rokni, K., Ahmad, A., Selamat, A., & Hazini, S. Water Feature Extraction and Change Detection Using Multitemporal Landsat Imagery. *Remote Sensing*, **2010**, *6*, 4173–4189. https://doi.org/10.3390/rs6054173.
7. Sarp, G., Ozcelik, M. Water body extraction and change detection using time series: A case study of Lake Burdur, Turkey. *Journal of Taibah University for Science*, **2017**, *11*, 381–391. https://doi.org/10.1016/j.jtusci.2016.04.005.
8. Mahdavi, S., Salehi, B., Granger, J., Amani, M., Brisco, B., Huang, W. *Remote sensing for wetland classification: A comprehensive review*. https://doi.org/10.1080/15481603.2017.1419602.
9. Gallant, A.L. The Challenges of Remote Monitoring of Wetlands. *U.S. Geological Survey*, **2015**, *7*, 10938–10950. https://doi.org/10.3390/rs70810938.
10. Rundquist, D.C., Narumalani, S., Narayanan, R.M. *A review of wetlands remote sensing and defining new considerations*. **2001**, *20*, 207–226. https://www.tandfonline.com/doi/pdf/10.1080/02757250109532435.
11. Lefebvre, G., Davranche, A., Willm, L., Campagna, J., Redmond, L., Merle, C., Guelmami, A., Poulin, B. Introducing WIW for detecting the presence of water in wetlands with landsat and sentinel satellites. *Remote Sensing*, **2019**, *11*. https://doi.org/10.3390/RS11192210.
12. Ramm, F. *OpenStreetMap Data in Layered GIS Format*. www.openstreetmap.org.
13. Shoop, S., Affleck, R., Collins, C., Larsen, G., Barna, L., Sullivan, P. Maneuver analysis methodology to predict vehicle impacts on training lands. *Journal of Terramechanics*, **2005**, *42*, 281–303.
14. Baylot, E.A., Gates, B.Q., Green, J.G., Richmond, P.W., Goerger, N.C., Mason, G.L., Cummins, C.L., Bunch, L.S. *Standard for Ground Vehicle Mobility*. 2005. https://citeseerx.ist.psu.edu/document?repid=rep1&type=pdf&doi=796fc644c30bea2e0109b3b0e1c939ed1cd27fcf
15. Suvinen, A. (n.d.). Terrain Mobility Model and Determination of Optimal off-Road Route.
16. Suleimenova, D., Bell, D., Groen, D. A generalized simulation development approach for predicting refugee destinations. *Scientific Reports*, 2017, *7*. https://doi.org/10.1038/s41598-017-13828-9.
17. Suleimenova, D., Groen, D. How policy decisions affect refugee journeys in South Sudan: A study using automated ensemble simulations. *Jasss*, **2020**, *23*. https://doi.org/10.18564/jasss.4193.